Check for updates

Journal of Intelligent Material Systems and Structures

Special Issue Article: ERMR2016 - Magnetorheological Fluids

Journal of Intelligent Material Systems and Structures
2018, Vol. 29(1) 32–40
© The Author(s) 2017
Reprints and permissions:
sagepub.co.uk/journalsPermissions.nav
DOI: 10.1177/1045389X17698248
journals.sagepub.com/home/jim
SAGE

Colloidal and viscoelastic properties of expanded perlite dispersions

Mehmet Cabuk[1], Tolga Acar Yesil[1], Mustafa Yavuz[1] and Halil Ibrahim Unal[2]

Abstract

In this study, structural properties of unexpanded perlite and expanded perlite particles were characterized using Fourier transform infrared spectroscopy, scanning electron microscopy, and thermogravimetric analysis techniques. Electrokinetic properties of unexpanded perlite and expanded perlite particles in polar (water) and non-polar (silicone oil) media were determined using zeta (ζ)-potential measurements as functions of time, pH, valences of electrolytes, type of surfactants, and temperature. Antisedimentation stabilities of the unexpanded perlite and expanded perlite particles dispersed in silicone oil were determined as a function of temperature at various volume fractions (ϕ = 5%−25% v/v). Viscoelastic properties of expanded perlite particles dispersed in silicone oil were investigated by creep and creep-recovery tests under externally applied electric field strengths. As a result, the ζ-potential and antisedimentation stability values revealed that colloidal stabilities of the expanded perlite particles were high enough to be used as smart electro-rheological material in long time durations. Expanded perlite/silicone oil dispersion behaved as a viscoelastic material and exhibited a reversible nonlinear viscoelastic deformation under applied electric field and showed a vibration damping capability for potential industrial applications.

Keywords

Unexpanded perlite, expanded perlite, zeta potential, colloidal stability, viscoelastic deformation

Introduction

Perlite is a glassy volcanic rock, commonly light gray, with a rhyolitic composition and 2%–5% of combined water. Commercially, the term perlite includes any volcanic glass that will expand or "pop" when heated quickly, forming a lightweight frothy material. The temperature at which expansion takes place ranges from 760°C to 1100°C; a voluminous increase of about 20 times is common, and it is named as "expanded perlite." Turkey possesses about 70% of the world's known perlite reserves (Demirbas et al., 2002). As most perlites have high silica content, usually greater than 70%, and are adsorptive; they are chemically inert in many environments and hence are excellent filter aids and fillers in various processes and materials (Alkan and Dogan, 1998; Leroy and Revil, 2004). Due to its structural properties, chemical compositions, and surface chemical properties, perlite has recently attracted much interest and has been intensively studied and widely used in many industrial products and processes (Alkan et al., 2005a).

In a study, acid-activated perlite samples were prepared from expanded perlite (EP) and unexpanded perlite (UEP), and their cation exchange capacities, densities, and specific surface areas were determined (Dogan and Alkan, 2004).

The electrokinetic measurement is one of the useful tools to enlighten the colloidal stability of dispersions and can be used to estimate the effect of the particle surface charge on aggregation behavior, flow, sedimentation, and filtration. Surface electric properties of colloidal particles can be altered by changing pH and ionic strength of the media (López-León et al., 2006; Unal et al., 2012). The ζ-potential is defined as the difference in electrical potential between the shear plane of a colloidal particle and the bulk of the solution (Rytwo et al., 2014).

[1]Department of Chemistry, Faculty of Science, Süleyman Demirel University, Isparta, Turkey
[2]Smart Materials Research Lab, Department of Chemistry, Faculty of Sciences, Gazi University, Ankara, Turkey

Corresponding author:
Mehmet Cabuk, Department of Chemistry, Faculty of Science, Süleyman Demirel University, 32260 Isparta, Turkey.
Email: mehmetcabuk@sdu.edu.tr; mhmtcbk@gmail.com

Electrorheological (ER) fluids are composed of polarizable particles dispersed in a non-polar fluid and regarded as smart materials because their flow behaviors can be tuned by externally applied electric field (E). Upon the application of an E, chain-like or fibrillar aggregates of the suspended particles are oriented along the direction of E, thereby inducing viscoelasticity and a drastic increase in viscosity (Kim et al., 2013; Prekas et al., 2013). Relatively little attention has been paid to the deformational (creep) response which can provide insight into the mechanistic origin of the flow of ER fluids. It is known that the creep and creep-recovery behaviors of ER fluids depend on dopant type and level, amount of applied stress, magnitude of E strength, and dispersed particle concentration (Liu and Choi, 2012). Viscoelastic behavior is one of the very important parameters for the materials in terms of reusability in industrial applications and can be elucidated by creep and creep-recovery tests (Cabuk et al., 2015; Chotpattananont et al., 2006).

There are only limited number of studies on perlite in the technical literature. Benefit of using environmental-friendly perlite as a dispersed phase in electrokinetic and ER applications is important from both industrial and environmental point of views. Because of the negative surface charge, ultralight weight, and porous structure of EP, it was aimed to investigate its electrokinetic and viscoelastic properties as a new smart material. In order to obtain information about the electrical state of the ionizable groups on the EP particle surfaces, electrokinetic properties in aqueous and non-polar silicone oil (SO) media were fully investigated as functions of pH, various electrolytes, surfactants, and temperature. Finally, viscoelastic behavior of the expanded perlite/silicone oil (EP/SO) dispersion was first examined by creep and creep-recovery tests as a function of applied E.

Experimental

Materials

The UEP and EP samples were obtained from AKPER Company (Çankırı, Turkey). The chemical composition of the perlite is shown in Table 1. Before the experiments, both samples were washed with distilled water to remove any impurities. Then, the particles were dried and ground milled using a Retsch MM400 model milling machine (Germany) to obtain homogeneous and finely distributed particles. SO ($\eta = 4.57 \times 10^{-3}$ Pa s, used in ζ-potential measurements; $\eta = 1.0$ Pa s, $\rho = 0.965$ g cm^{-3}, and $\varepsilon = 2.61$ at 25°C, used in creep-recovery tests) were obtained from Aldrich. NaCl, $BaCl_2$, $MgSO_4$, Na_2SO_4, and $AlCl_3$ used as electrolytes; cetyltrimethylammonium bromide (CTAB), sodium dodecyl sulfate (SDS), and Triton X-100 (Triton-X) used as surfactants in electrokinetic studies were analytical grade obtained from Merck (Germany). All the other chemicals were purchased from Aldrich with analytical grade and used as received without further purification.

Table 1. Chemical composition of perlite (Alkan and Dogan, 1998).

Component	%
SiO_2	72−76
Al_2O_3	11−17
K_2O	4−5
Na_2O	3−4
CaO	0.5−2
MgO	0.1−0.5
Fe_2O_3	0.5−1.5
TiO_2	0.03−0.2
MnO_2	0.03−0.1
SO_3	0−0.2
H_2O	2−7

Characterizations

Perkin Elmer Spectrometer BX model (England) was used to record the Fourier transform infrared spectroscopy (FTIR) spectra of UEP and EP particles as KBr disks. Morphologies of the samples were examined using a scanning electron microscope (JEOL JSM 5500LV, Tokyo, Japan). Thermal behaviors of the samples were performed with a Perkin Elmer Diamond TGA/DSC thermal analysis instrument (USA). The specimens were heated at a rate of 10°C min^{-1} under N_2 atmosphere from room temperature to 600°C.

Antisedimentation stability measurements

Colloidal dispersions of the UEP and EP particles were prepared in SO at different volume fractions ($\phi = 5\%-25\%$ v/v). To measure the colloidal stabilities of these dispersions under various environmental conditions, antisedimentation stability values against gravitational forces were determined at four different temperatures (−20°C + 1°C + 25°C, and 40°C) for a period of 30 days. For this, glass tubes containing the dispersions were immersed into a constant temperature water bath, and formation of the first precipitates was recorded to be the indication of colloidal instability. During the neat eye observations, the height of phase separation between the particle-rich phase and the relatively clear oil-rich phase was recorded as a function of time using a digital composing stick. The antisedimentation ratio was defined as the height of the particle-rich phase divided to the total height of dispersion.

Electrokinetic measurements

ζ-potential measurements were performed with a Malvern Zetasizer Nano ZS, which works with laser Doppler electrophoresis technique using folded capillary cell equipped with gold electrodes. The optic unit contains a 4-mW He–Ne laser ($\lambda = 633$ nm). The self-optimization routine in the Zetasizer software was used for all the measurements. The waiting time before the measurements was 2 min. The ζ-potential value was calculated from the electrophoretic mobility of particles using Henry's equation

$$\zeta = \frac{3\eta U_E}{2\varepsilon f(\kappa\alpha)} \quad (1)$$

where U_E is the electrophoretic mobility ($m^2\ V^{-1}\ s^{-1}$); ε is permittivity of the medium ($F\ m^{-1}$); η is the viscosity of medium ($N\ m^{-2}\ s$); $f(\kappa\alpha)$ is Henry's function, which depends on the particle size and shape; κ is the reciprocal of EDL thickness; the Debye length (m^{-1}); and α is the particle radius (m). Two values are generally used as approximations for $f(\kappa\alpha)$ determination (either 1.5 or 1.0). $f(\kappa\alpha)$ in this case is 1.5 and is referred to as the Smoluchowski approximation. The Hückel equation is an approximation valid for non-polar medium (i.e. SO). $f(\kappa\alpha)$ in this case is 1.0.

Preparation of the EP dispersions in water and SO media

To determine the electrokinetic properties of the UEP and EP particles, 0.1 g L^{-1} colloidal dispersions were prepared in deionized water. Then, the dispersions were subjected to sonication for 30 min and held at room temperature for further 20 min to establish equilibrium and to reach $pH_{relaxation}$. Afterwards, the supernatant liquid was used for the ζ-potential measurement and the pH was adjusted immediately by an MPT-2 autotitrator unit at 25°C. The effects of pH, NaCl, $BaCl_2$, $MgSO_4$, Na_2SO_4, and $AlCl_3$ electrolytes; various surfactants (cationic: CTAB; anionic: SDS and nonionic: Triton X-100); and temperature on the ζ-potentials of the dispersions were investigated and then the colloidal stabilities determined. Additionally, ζ-potentials of the particles dispersed in non-polar SO at 0.2 g L^{-1} concentration were measured using a dip cell and calculated according to the Hückel approximation.

Creep and recovery measurements

To measure the viscoelastic properties of the EP particles via creep and creep-recovery tests, Thermo-Haake RS600 parallel plate torque electrorheometer (Germany) was used with a 35-mm plate-to-plate geometry. The voltage used in the viscoelastic experiments was supplied by a 0−12.5-kV (with 0.5 kV increments) DC external E generator (FUG Electronics, Germany), which enabled resistivity to be created during the experiments.

During the creep-recovery experiment, a constant stress ($\tau = 20$ Pa) was applied instantaneously ($t = 30$ s) to EP/SO dispersion ($\phi = 10\%$ v/v) under $E = 0$ and $E \neq 0$ conditions, and changes in strains (γ) were measured over a period. Then, the stress was set to $\tau = 0$ Pa, and with this measurement, the recoverable elastic portion of the deformation was determined.

Results and discussions

Characterization results

The FTIR spectra of UEP and EP samples were depicted in Figure 1. Both samples show characteristic peaks which are typical clay peaks at almost same wavelengths. Because of the expansion in the EP structure, the peak intensities were observed to increase. The broad band between 3450 and 3600 cm^{-1} is attributed to stretching vibrations of surface –OH groups of –Si–OH. The peaks at 1600 cm^{-1} were attributed to bending mode of O–H arising from water molecules. The intense peaks at 1050 cm^{-1} were due to the stretching vibrations of Si–O–Si structures. The peaks at around 800 and 450 cm^{-1} are assigned to stretching vibrations of Si–O and Al–O, respectively. Similar results were reported for the immobilization of copper nanoparticles on perlite in the literature (Nasrollahzadeh et al., 2015).

The scanning electron microscopy (SEM) images of UEP and EP particles are given in Figure 2. It was observed that both particles have different morphologies. UEP particles have tight and nonporous surface morphology. When it expands to form EP particles, very porous and homogeneous spongy-like structures form. Similar pattern was observed for other reported micrographs of perlite in the literature (Lu et al., 2014).

Figure 3 illustrates the TGA curves of UEP and EP particles between 25°C and 600°C. The first step around 30°C−100°C with 1% weight loss is attributed to the removal of moisture and breaking of H-bonds between

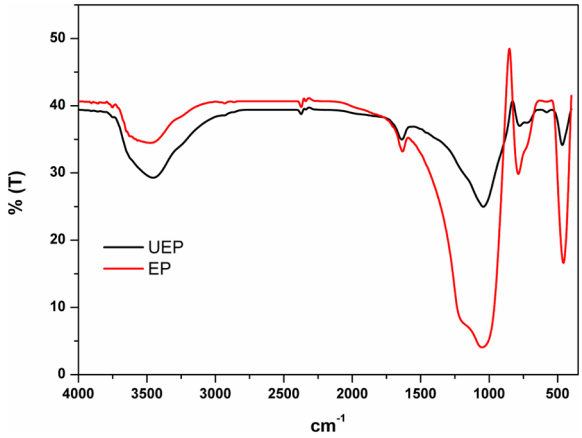


Figure 1. FTIR spectra of the UEP and EP particles.

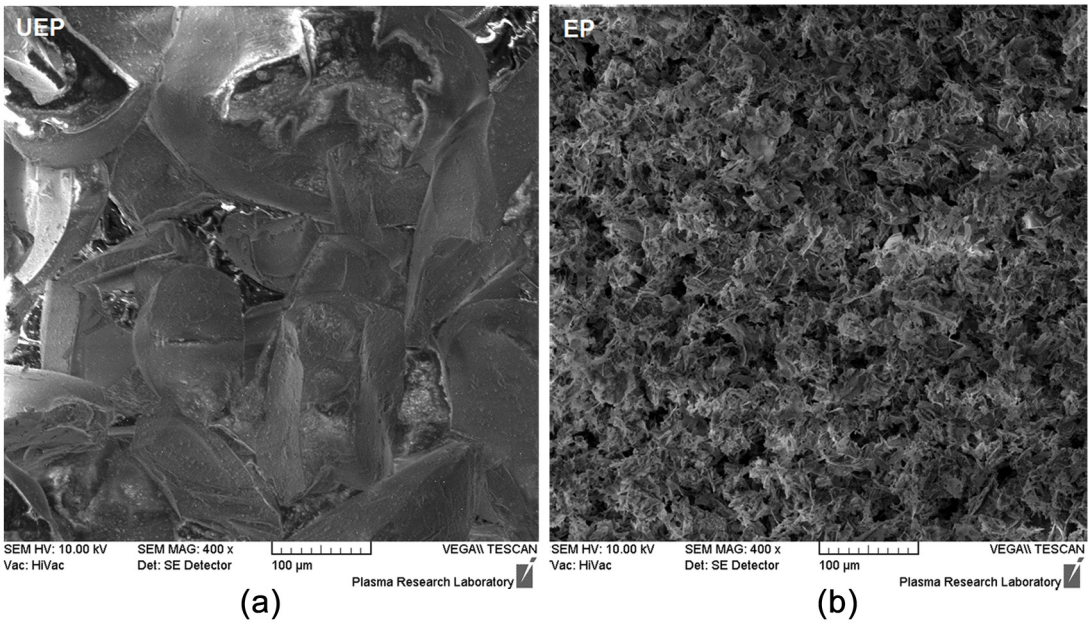


Figure 2. SEM images of (a) UEP and (b) EP particles.

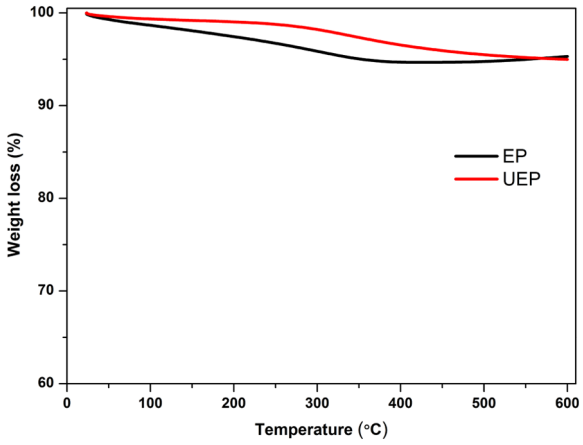


Figure 3. TGA curves of the UEP and EP particles.

water and silicate chains. The second step around 200°C−500°C with 5% weight loss is due to thermal decomposition of perlite structure. Thermal stabilities of the UEP and EP particles at the end of 600°C were found as 95%. It was noticed that the weight loss was faster in EP, which was attributed to the expansion of the silicate layers which results with the fast distribution of temperature. It was concluded that the thermal stabilities of the samples were suitable for high-temperature ER applications.

Antisedimentation stability results

Antisedimentation stability is one of the critical parameters desired for good electrokinetic and viscoelastic studies. In these studies, long-term colloidally stable dispersions in challenging environmental conditions are desired. The particles with micron size in a dispersion settle down according to Stoke's law (Uemura et al., 1995).

Table 2. Antisedimentation stability ratios of EP/SO dispersions at the end of 30 days.

Φ (v/v)	Temperature of the environment			
	−20°C	1°C	25°C	40°C
5	92	94	68	63
10	94	96	73	70
15	96	97	77	73
20	97	97	80	78
25	98	98	81	81

EP/SO: expanded perlite/silicone oil.

In this study, effects of temperature and dispersed particle volume fractions on the antisedimentation ratios of the dispersions were examined and results obtained are given in Table 2. It was observed that the UEP dispersions showed immediate aggregation on the first day of the experiment. However, EP/SO dispersions showed extremely high antisedimentation stabilities. That is why, just EP/SO dispersions were used for the rest of electrokinetic and viscoelasticity measurements.

Increasing antisedimentation ratios were recorded with decreasing temperature. It can be attributed to increasing viscosity of SO media. However, when the effect of dispersed-phase volume fraction was considered, it was observed that antisedimentation ratios of the EP/SO dispersions were increased with increasing

dispersed-phase volume fraction. This was attributed to the enhanced repulsive forces acting between the dispersed particles with increasing volume fractions. While the minimum antisedimentation ratio of EP/SO dispersion was obtained as 63% at 5% volume fraction and +40°C, the maximum antisedimentation ratio was recorded as 98% at a volume fraction of 25% and −20°C. Generally, these results are reliable for a colloidally stable dispersion in terms of potential industrial applications.

Electrokinetic results in aqueous medium

The electrokinetic properties of the EP particles were determined by ζ-potential measurements and results obtained are discussed below.

Effect of pH on ζ-potentials

Surface hydroxyl groups of perlite can be protonated or deprotonated in acidic or basic media. Therefore, ζ-potential of perlite dispersions can be determined as a function of pH. By this method, ζ-potential can pass through a net zero point of charge, which is called isoelectric point (IEP). IEP value indicates that total positive charges on particles are equal to the total negative charges; hence, particles are colloidally unstable. For a physically stable dispersion solely stabilized by electrostatic repulsions, a ζ-potential of ± 30 mV is preferred as minimum. In Figure 4, ζ-potential of EP particles is plotted as a function of pH at a constant ionic strength (1×10^{-3} M NaCl). EP dispersions were stable at the initial equilibrium condition (−36 mV at pH = 4.5). This negative ζ-potential value may be due to isomorphic transactions (Alkan et al., 2005b) and structural –OH groups ($-SOH + OH^- \rightarrow SO^- + H_2O$).

When the $HCl_{(aq)}$ solution is added into the $EP_{(aq)}$ dispersion, concentration of $[H_3O^+]$ ions in the dispersion proportionally increases with the changing pH from initial to 3. An electrostatic interaction between negatively charged EP surface and H_3O^+ ions occurs and lead to the protonation of OH^- groups of the EP surfaces. Therefore, negative ζ-potential values of the EP dispersions decreased and stayed in negative region with the decrease in dispersions' pH values (Figure 4). The lowest ζ-potential value was obtained at pH = 3 as −21 mV.

When the $NaOH_{(aq)}$ solution is added into the EP dispersion, concentration of $[OH^-]$ increases with the increasing pH value from initial to 11. This can lead to selective adsorption of OH^- anions on the surfaces of EP particles. As a result, ζ-potential of the EP dispersion shifts to more negative regions with increasing pH value. The highest ζ-potential value was observed at pH = 11 as −66 mV. It is known that for the clay kind materials, potential determining ions are $(H_3O)^+$ and OH^- ions. These potential determining ions control the surface electrokinetic reactions. It is clearly seen that $EP_{(aq)}$ dispersion is generally in colloidally stable range at the studied pH conditions. The reason of the changing ζ-potential of perlite particles with pH may be due to the ionization of silanol groups on perlite surface, and these silanol groups complete their coordination with OH groups. There are more silanol groups in the EP structure than unexpanded one, because of the broken structural edges by heating. With the high negative surface charge, EP particles can proposed as a new colloidally stable potential ER-active material.

Effect of various electrolytes on ζ-potentials

With the increasing valency of the electrolytes, colloidal stability of dispersion can be altered. Figure 5 shows the effects of valencies of various cations and anions on the ζ-potential of $EP_{(aq)}$ dispersion at a constant concentration. When H_3O^+ cations or OH^- anions were added gradually into the dispersion medium,

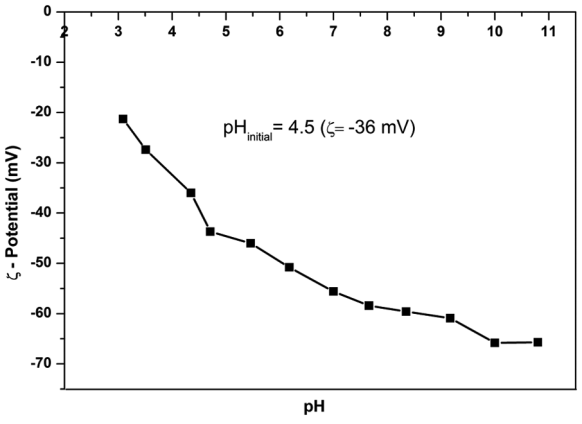


Figure 4. The effects of pH on ζ-potentials of EP dispersions, c_{sample} = 0.1 g L^{-1} and T = 25°C.

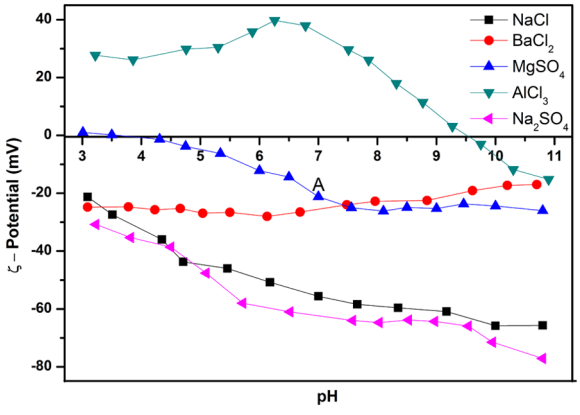


Figure 5. The effects of various electrolytes on ζ-potentials of EP dispersions, c_{sample} = 0.1 g L^{-1}, c_{salt} = 1 × 10^{-3} M, and T = 25°C.

ζ-potential of the dispersions shifted to more positive and negative regions, respectively. The shifts to the positive ζ-potential region are dominant when the valencies of the cations increased from $+1$ (Na^+) to $+2$ (Ba^{2+} and Mg^{+2}) and $+3$ (Al^{3+}). However, when the valencies of the anions increased from -1 (Cl^-) to -2 (SO_4^{2-}), shifts to more negative region are dominant. The radius of ions is effective for the ions to approach onto the particles' surfaces. Therefore, the ions which has smallest radius, strongly interact with the surface groups. The larger ions tend to distort easily. Because of the Coulombic attraction (Chapman, 1965), these kinds of ions are called counter ions and accumulate in electrical double layer (EDL). Hence, they compress the thickness of EDL and cause to change ζ-potential of EP particles.

The results obtained can be supported with following equation (2)

$$\kappa^{-1} = \frac{0.3041}{Zc^{1/2}} \quad (2)$$

where κ^{-1} is the Debye length, which is a measure of the EDL thickness. As shown, κ^{-1} is related to the valency of the ion (Z) and ion concentration (c) in a dispersion (Kitahara and Watanabe, 1984). According to this formula, at the constant electrolyte concentration, κ^{-1} value decreases with increasing valencies of the ions and consequently causes a reduction in the ζ-potential. The values of κ^{-1} of EP dispersions were determined to change in the following order at 1×10^{-3} M electrolyte concentrations: $\kappa^{-1}_{Al^{3+}} = 3$ nm $< \kappa^{-1}_{Ba^{2+}} = \kappa^{-1}_{Mg^{2+}} = \kappa^{-1}_{SO_4^{2-}} = 5$ nm $< \kappa^{-1}_{Na^+} = \kappa^{-1}_{Cl^-} = 10$ nm.

It was concluded that due to the presence of negatively charged –OH groups on the surfaces of EP particles, presence of cationic electrolytes caused instable colloidal dispersions by reducing the ζ-potentials while anionic electrolytes helped the formation of colloidally stable dispersions by shifting the ζ-potentials to more stable regions.

Effect of surfactants on ζ-potentials

The adsorption of surfactants on a solid particle surface depends on various factors such as structure of solid particle surface, structure of surfactant, and environment of dispersion media (pH, temperature, and salts; Alkan et al., 2005b). Figure 6 shows the changes in ζ-potentials of $EP_{(aq)}$ dispersion as a function of cationic (CTAB), anionic (SDS), and nonionic (Triton X-100) surfactant concentrations ($c_{Surfactant} = 0 - 20$ ppm). It was observed that $EP_{(aq)}$ colloidal dispersion has a negatively charged surface at the absence of CTAB. When cationic CTAB was added into $EP_{(aq)}$ colloidal dispersion, negative surface charge of the EP particles decreased, and at higher concentrations than 10 ppm, ζ-potential value shifted to positive values ended up

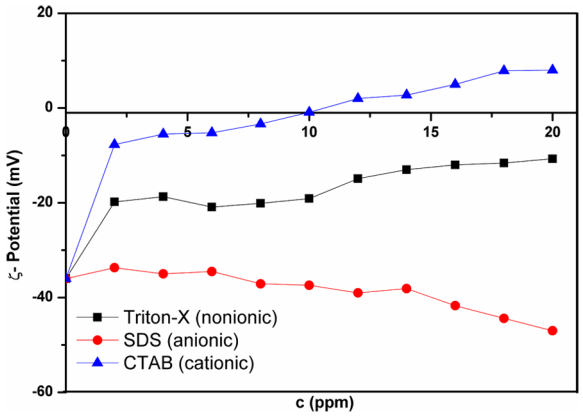


Figure 6. The effects cationic, anionic, and nonionic surfactants on ζ-potential of EP dispersions, c_{sample} = 0.1 g L^{-1}, $c_{surfactant}$ = 0–20 ppm, and T = 25°C.

with $+8$ mV at $c_{CTAB} = 20$ ppm. EP particles have high negative surface charge because of the silanol groups. Therefore, with the increasing CTAB concentration, cationic CTAB tails are adsorbed by these silanol groups. Then, the surface of EP neutralized and surface charge changed. In a study, adsorption properties of UEP and EP samples in aqueous CTAB solutions were investigated. It was reported that the sorption capacity of the samples increased with increasing ionic strength and pH and decreasing temperature (Alkan et al., 2005b).

However, with the addition of an anionic SDS surfactant, the surface coverage of EP particles increased with an increasing negatively charged SDS concentration. The interactions between the SDS molecules and the EP surfaces are cooperative and mainly hydrophobic since sign of the both surfaces are the same. It was observed that ζ-potential of EP particles shifted more positive values and ended up with -48 mV at $c_{SDS} = 20$ ppm, without passing through an IEP.

With the addition of nonionic surfactant Triton-X into the EP dispersion, negatively charged EP surfaces were covered by nonionic surfactant molecules and caused to decrease the surface charge. Therefore, the negative ζ-potential value of EP particles slightly decreased and ended up with -10 mV at $c_{SDS} = 20$ ppm. Also, Triton-X molecules do not dissociate in water and can exhibit weakly charged dipoles due to their polarity. Therefore, they may cause slight decrease in ζ-potential value. These results revealed that with the addition of cationic, anionic, or nonionic surfactants into the $EP_{(aq)}$ dispersion, colloidal stability of the dispersion can be adjusted.

Effect of temperature on ζ-potentials

Temperature is an important factor affecting the colloidal stability of dispersion. Figure 7 shows the effect of

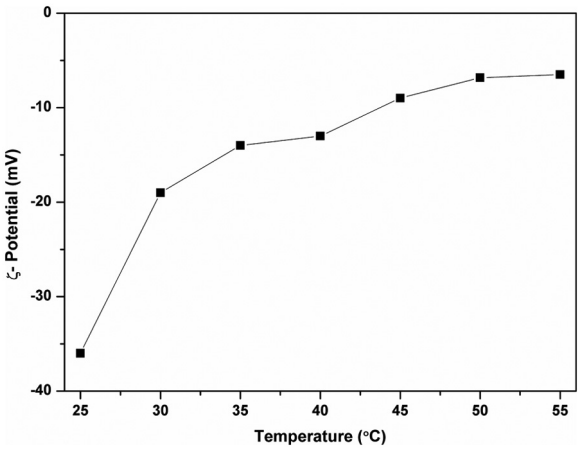


Figure 7. The effect of temperature on ζ-potential of EP dispersions, c_{sample} = 0.1 g L^{-1}.

temperature on ζ-potential onto EP dispersion. As seen that with rising temperature from 25°C to 55°C, ζ-potential values of EP particles decreased from −18 to −7 mV. This decreasing trend of ζ-potential can be attributed to desorption of negatively charged ions from the particle surface. The increase in desorption (or decrease in adsorption) of ions with increasing temperature at constant electrolyte concentration depends on the structure of surface and solution (Juang et al., 1997). For the EP dispersion system, desorption may be comparatively stronger than adsorption. However, the mobility of the particles increases with increasing temperature, since the ionic mobility increases and viscosity decreases at higher temperatures (Hsu et al., 2012). Therefore, the diffuse layer around dispersed particles cannot establish and cause decrease in ζ-potential value of EP dispersion.

ζ-potential in non-polar medium

The rheological properties of a colloidal dispersion are closely associated with the surface chemistry of the dispersed particles (Uhlherr et al., 2005). To prepare colloidally stable ER-active fluids from the particles, we need to determine their colloidal stabilities in non-polar SO medium by ζ-potential measurements. ζ-potentials in non-polar medium have been extensively studied for electrophoretic display applications (Park et al., 2012). The ζ-potential value of EP/SO dispersion was measured as −42 mV. As seen that the ζ-potential value was in the colloidally stable range and suitable for potential viscoelastic ER measurements. It is well known that electrophoretic mobility of dispersed particles in non-polar medium is restricted; ζ-potential measurement become possible with the polarizability of absorbed or adsorbed moisture from the environment onto the surfaces of particles by triggering the interparticle interactions.

Viscoelasticity results

Viscoelastic property of materials can be measured via creep and creep-recovery tests, which is one of the very important parameters for materials in terms of reusability in industrial applications (Koyuncu et al., 2011). As schematically given in Figure 8, the creep test is characterized by two distinct phases as the creep phase and the recovery phase (Erol et al., 2013; Vicente et al., 2001). First, in the creep phase, strain (γ) of a viscoelastic material increases with time under sustained stress. Then, in the recovery phase, when the applied stress is removed, the time-dependent strains can be recoverable with time. Viscoelastic materials behave in two different ways in the recovery phase: (1) in the nonlinear viscoelastic behavior, some of the deformations are recovered and (2) in linear viscoelastic behavior, in which all of the creep phase deformations can be recoverable. For a viscoelastic material, in general, the time dependence of the strain $\gamma_C(t)$ can be expressed in terms of three contributions

$$\gamma_C(t) = \gamma_s + \gamma_d(t) + \gamma_v(t) \tag{3}$$

where γ_s is the instantaneous strain, for a linear viscoelastic material, $\gamma_d(t)$ is the retardation strain which describes a delayed elastic response, requiring time to develop fully, and $\gamma_v(t)$ is the viscous flow or the irreversible component of strain.

The creep and recovery response of EP/SO dispersion prepared at 10% volume fraction were determined with the presence ($E \neq 0$ kV mm^{-1}) and absence ($E = 0$ kV mm^{-1}) of E and results obtained are depicted in Figure 8. For the $E = 0$ kV mm^{-1} condition, EP/SO dispersion behaved as purely viscous material under 20 Pa of stress and any recovered deformation was not observed. When the applied stress was removed ($\tau = 0$ Pa), the recovery of creep was not observed, and the dispersion exhibited viscous flow. It was concluded that the deformation was purely viscous and permanent after the stress was removed and larger in the creep phase due to the weak electrostatic interactions of dispersed EP particles in SO media. When E was applied to the EP/SO dispersion, some deformations were recovered and the dispersion behaved as viscoelastic material. This may be attributed to the formations of chain-like or fibrillar structures of the polarized EP particles in the dispersion.

The creep curves under applied stress ($\tau = 20$ Pa) comprised three steps: the instantaneous strain, the retardation strain, and the viscous strain. In the creep phase, a decrease in the instantaneous strain (γ_s) can be clearly observed with the increase in E strength. The instantaneous strain values of EP/SO dispersion were found to be in the following order: $\gamma_s = 1.81 \times 10^{-5} < \gamma_s = 2.57 \times 10^{-5} < \gamma_s = 3.15 \times 10^{-5}$ for $E =$ 3, 2, and 1 kV mm^{-1} conditions, respectively. After the applied stress was removed, the recovery curve was

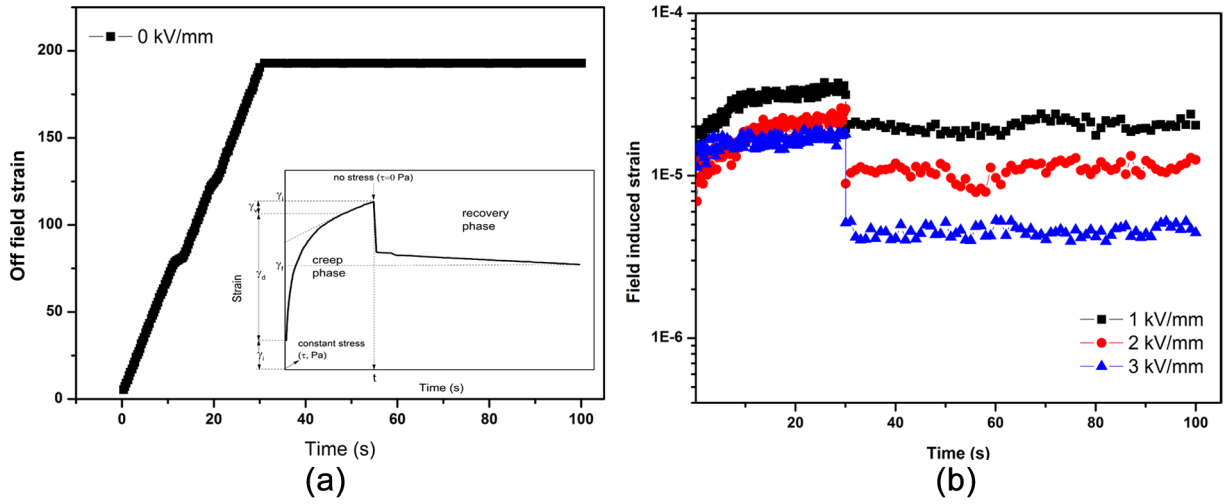


Figure 8. Creep and recovery behavior of EP/SO dispersion under (a) E = 0 and (b) E = 1, 2, and 3 kV mm^{-1} conditions, ϕ = 10% v/v, and T = 25°C. Inset schematic representation of the creep and recovery response under a constant applied stress for a nonlinear viscoelastic material ($E \neq 0$ kV mm^{-1} condition).

determined until t = 70 s. EP/SO dispersion showed an instantaneous elastic recovery (γ_r) and then slower recovery steps. The recovery values of the materials increased with increasing E (from 1 to 2 kV mm^{-1}). This may be attributed to the formation of stronger chain-like structures of the polarizable negatively charged EP particles in the suspension at elevated E. These polarizable particles could be re-oriented and chain-like structures could be formed, which enhances the ER activity. Similar viscoelastic deformation behavior was reported for chitosan/high-density polyethylene (HDPE) suspensions (Mir et al., 2011). In another study on rheological and electrokinetic properties of sodium montmorillonite suspensions, the yield stress decreases up to an order of magnitude between pH 3 and 7, with a much slower rate of decrease in the 7–11 pH interval. Creep-recovery measurements demonstrate that the behavior of the suspensions is more elastic than viscous one (storage modulus larger than loss modulus), mainly in the acidic pH range (Duran et al., 2000).

The percentage recoverable strains (RS) of EP/SO system were calculated from the equation (Cho et al., 2004)

$$RS(\%) = \left(\frac{\gamma_i - \gamma_f}{\gamma_i}\right) \times 100 \qquad (4)$$

where γ_i is the total strain acquired before removing the applied stress and γ_f is the average steady state strain after removing the applied stress. RS of EP/SO ER fluid were observed as following: $RS_{E=0} = 0\% < RS_{E=1} = 35\% < RS_{E=2} = 51\% < RS_{E=3} = 75\%$. This may be attributed to the higher polarizability of the particles which create stronger fibrillar aggregates due to negatively surface charge of perlite in SO. According to the % recovery values of the dispersion, EP/SO system behaved as smart viscoelastic material under E-induced conditions.

Conclusion

Structural and morphological properties of UEP and EP particles were characterized using FTIR, SEM, and TGA techniques. Electrokinetic results in aqueous medium revealed that negative ζ-potential of EP dispersion (−36 mV) was found to be in the colloidally stable region at all the pH ranges. The ζ-potential value can be altered by the changing valencies of electrolytes, kind of surfactants, and temperature of the dispersion medium. While the surface charge of the EP particles shifted to positive region with the presence of $AlCl_3$ salt, the surface charge stayed at negative region with the addition the other electrolytes. ζ-potential value (−42 mV) in the non-polar medium revealed that colloidal stabilities of the particles were high enough to be used as a new viscoelastic ER-active smart material. Viscoelastic results revealed that while nonlinear recoverable viscoelastic creep behavior (elastic response) was observed under E-induced condition, unrecoverable viscoelastic creep behavior (viscous fluid) were observed without E. Hence, we suggest that the natural EP particles with high colloidal stability and viscoelastic response could be a good candidate as a new smart material for industrial vibration damping applications.

Declaration of Conflicting Interests

The author(s) declared no potential conflicts of interest with respect to the research, authorship, and/or publication of this article.

Funding

The author(s) disclosed receipt of the following financial support for the research, authorship, and/or publication of this article: The authors thank the TÜBİTAK (Grant no. 214Z199) for the financial support of this work.

References

Alkan M and Dogan M (1998) Surface titrations of perlite suspensions. *Journal of Colloid and Interface Science* 207: 90–96.

Alkan M, Demirbas O and Dogan M (2005a) Zeta potential of unexpanded and expanded perlite samples in various electrolyte media. *Microporous and Mesoporous Materials* 84: 192–200.

Alkan M, Karadas M, Dogan M, et al. (2005b) Adsorption of CTAB onto perlite samples from aqueous solutions. *Journal of Colloid and Interface Science* 392: 75–82.

Cabuk M, Yavuz M and Unal HI (2015) Colloidal, electrorheological, and viscoelastic properties of polypyrrole-graft-chitosan biodegradable copolymer. *Journal of Intelligent Material Systems and Structures* 26(14): 1799–1810.

Chapman HD (1965) *Methods of Soil Analysis, Chemical and Microbiological Properties*. Madison, WI: American Society of Agronomy, pp. 891–901.

Cho MS, Lee JH, Choi HJ, et al. (2004) Linear viscoelasticity of semiconducting polyaniline based electrorheological suspensions. *Journal of Materials Science* 39: 1377–1382.

Chotpattananont D, Sirivat A and Jamieson A (2006) Creep and recovery behaviors of a polythiophene-based electrorheological fluid. *Polymer* 47: 3568–3575.

Demirbas O, Alkan M and Dogan M (2002) The removal of Victoria blue from aqueous by adsorption on a low-cost material. *Adsorption* 8: 341–349.

Dogan M and Alkan M (2004) Some physicochemical properties of perlite as an adsorbent. *Fresenius Environmental Bulletin* 13: 251–257.

Duran JDG, Ramos-Tejada MM, Arroyo FJ, et al. (2000) Rheological and electrokinetic properties of sodium montmorillonite suspensions: I. Rheological properties and interparticle energy of interaction. *Journal of Colloid and Interface Science* 229: 107–117.

Erol O, Ramos-Tejada MM, Unal HI, et al. (2013) Effect of surface properties on the electrorheological response of hematite/silicone oil dispersions. *Journal of Colloid and Interface Science* 392: 75–82.

Hsu JP, Tai YH and Yeh LH (2012) Importance of temperature effect on the electrophoretic behavior of charge-regulated particles. *Langmuir* 28: 1013–1019.

Juang RS, Wu FC and Tseng RL (1997) The ability of activated clay for the adsorption of dyes from aqueous solutions. *Environmental Technology* 18: 525–531.

Kim YJ, Liu YD, Choi HJ, et al. (2013) Facile fabrication of Pickering emulsion polymerized polystyrene/laponite composite nanoparticles and their electrorheology. *Journal of Colloid and Interface Science* 394: 108–114.

Kitahara A and Watanabe A (1984) *Electrical Phenomena at Interfaces Fundamentals, Measurements and Applications*. New York: Marcel Dekker.

Koyuncu K, Unal HI, Gumus OY, et al. (2011) Electrokinetic and electrorheological properties of poly(vinyl chloride)/polyindole conducting composites. *Polymers for Advanced Technologies* 23: 1464–1472.

Leroy P and Revil A (2004) A triple-layer model of the surface electrochemical properties of clay minerals. *Journal of Colloid and Interface Science* 270: 371–380.

Liu YD and Choi HJ (2012) Electrorheological fluids: smart soft matter and characteristics. *Soft Matter* 8: 11961–11978.

López-León T, Ortega-Vinuesa JL, Bastos-Gonzalez D, et al. (2006) Cationic and anionic poly(N-isopropylacrylamide) based submicron gel particles: electrokinetic properties and colloidal stability. *Journal of Physical Chemistry B* 110: 4629–4636.

Lu Z, Xu B, Zhang J, et al. (2014) Preparation and characterization of expanded perlite/paraffin composite as form-stable phase change material. *Solar Energy* 108: 460–466.

Mir S, Yasin T, Halley PJ, et al. (2011) Thermal, rheological, mechanical and morphological behavior of HDPE/chitosan blend. *Carbohydrate Polymers* 83: 414–421.

Nasrollahzadeh M, Sajadi SM, Rostami-Vartooni A, et al. (2015) Immobilization of copper nanoparticles on perlite: green synthesis, characterization and catalytic activity on aqueous reduction of 4-nitrophenol. *Journal of Molecular Catalysis A: Chemical* 400: 22–30.

Park BJ, Hong SY, Sim HH, et al. (2012) Effect of charge control agent on electrophoretic characteristics of polymer encapsulated titania nanoparticle. *Materials Chemistry and Physics* 135: 259–263.

Prekas K, Shah T, Soin N, et al. (2013) Sedimentation behaviour in electrorheological fluids based on suspensions of zeolite particles in silicone oil. *Journal of Colloid and Interface Science* 401: 58–64.

Rytwo G, Lavi R, König TM, et al. (2014) Direct relationship between electrokinetic surface-charge measurement of effluents and coagulant type and dose. *Colloids and Interface Science Communications* 1: 27–30.

Uemura T, Minagava K, Takimato J, et al. (1995) Opposite electrorheological effects between urethane-based polymers having different terminal groups. *Journal of the Chemical Society, Faraday Transactions* 91: 1051–1052.

Uhlherr PHT, Guo J, Tiu C, et al. (2005) The shear-induced solid–liquid transition in yield stress materials with chemically different structures. *Journal of Non-Newtonian Fluid Mechanics* 125: 101–119.

Unal HI, Sahan B and Erol O (2012) Investigation of electrokinetic and electrorheological properties of polyindole prepared in the presence of a surfactant. *Materials Chemistry and Physics* 134: 382–391.

Vicente J, Duran JDG and Delgado AV (2001) Electrokinetic and viscoelastic properties of magnetorheological suspensions of cobalt ferrite. *Colloids and Surfaces A: Physicochemical and Engineering Aspects* 195: 181–188.